1st IMEKO TC-4 International Workshop on
Metrology for Geotechnics
Benevento, Italy, March 17-18, 2016

Numerical interpretation of monitoring data of an instrumented tunnel segmental ring

Stefania Fabozzi[1], Emilio Bilotta[2], Gianpiero Russo[3]

[1] *University of Naples Federico II, via Claudio 21 – 80128 Napoli, Italy, stefania.fabozzi@unina.it*
[2] *University of Naples Federico II, via Claudio 21 – 80128 Napoli, Italy, emilio.bilotta@unina.it*
[3] *University of Naples Federico II, via Claudio 21 – 80128 Napoli, Italy, gianpiero.russo@unina.it*

***Abstract* – The segmental nature of the support system, the interaction mechanism between concrete-grout-soil and the complex installation process a bored tunnel are the main factors influencing the lining structural behavior. The main purpose of this study is to provide a two dimensional numerical model of segmental lining which takes into account the first two factors for the preliminary interpretation of the experimental data obtained by long-term monitoring of the strains in the instrumented segments of a precast segmental ring of Naples Metro Line 6. This model can be extended to three dimensions for a complete interpretation of monitoring data, including consideration of the tunnel excavation process.**

I. INTRODUCTION

The structural discontinuities that mark the transition between the segments in the same ring *(longitudinal joint systems*) and between the linings of adjacent rings (*transversal*, *circumferential or lateral joint systems*), have a double effect on the structural response of the lining support. The longitudinal joints implies a local stiffness reduction respect to the case of monolithic ring, circumferential joints, staggered along the tunnel axis, involve coupling effect between adjacent rings when they are subjected to longitudinal uniform load. In literature, the first effect is usually considered through indirect methods, which consider the presence of joints setting a reduced flexural rigidity of the continuous ring [1] or direct methods, modelling the joints as elements with own stiffness.

Joint connection's structural behavior is intermediate between a ideally fully rigid and a pinned connection [2]; the first condition implies the complete continuity between the connected segments, i.e. the complete transfer of forces between the two surfaces in contact, the second condition implies instead a rotational capability of the node that does not develop bending stresses. The intermediate behavior, generally classified as a semi-rigid connection, allows to the transfer of axial forces, shearing forces and bending moments. A semi rigid connection is most influenced by bending deformation than by axial and shear deformation. Hence a good approximation to model this behavior is to consider only the rotational deformation of the joint described by a nonlinear moment rotation curve (M-θ). Simplified numerical approaches model longitudinal joints behavior by means of rotational springs [3-4], more sophisticated methods better represent the real behavior of connection joints. Arnau et al. 2012 [5], for instance, modelled the longitudinal joints with non-linear interface elements behaving rigid in compression; Do et al. 2013 [6], represented instead the connection with rotational and radial springs modelled by means of a bi-linear relation M-θ and an elastic axial spring, respectively.

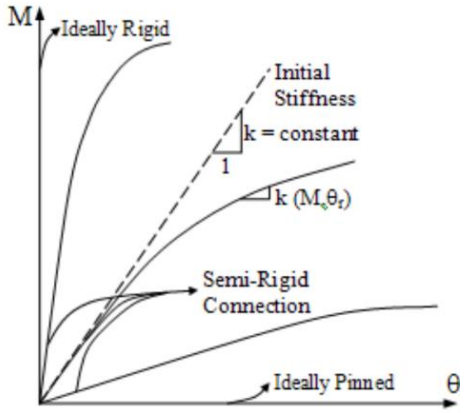

Fig. 1 Structural behaviour of connections [7].

II. SEGMENTAL LINING DESIGN

Nonlinear models are available in literature to simulate joint behavior considering only their bending moment transfer, while neglecting normal and shear components. Janssen's method [8], for instance, models the non-linear behavior of the joint with a rotational spring connecting the contact surface of two adjacent tunnel segment (Figure 2).

The concrete hinge method, according to Leonhardt

ISBN: 978-92-990075-0-1

and Reimann (1966) [9], models the contact area with a concrete beam with depth equal to the joint width t_j and height and width equal to the joint contact height.

(a) *(b)*

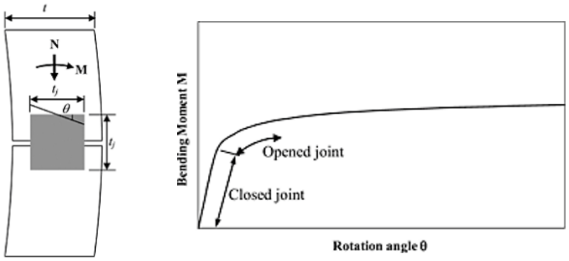

Fig. 2. (a) Cross section of the longitudinal joint; (b)M-θ relation of Janssen joint.

Opening of the joint is due to the fact that the concrete beam cannot resist any tensile stresses. As shown in Figure 2(b) a limit value of bending moment M exists under which the joint is fully compressed. The resulting force is inside the core section of joint and rotational stiffness is constant. Above this value, the joint is open and rotation θ increases until the joint has a fully plastic behavior.

This formulation has been used to calibrate the numerical model of longitudinal joint in Plaxis 2D in the form of a bilinear spring curve [10].

(a) (b)

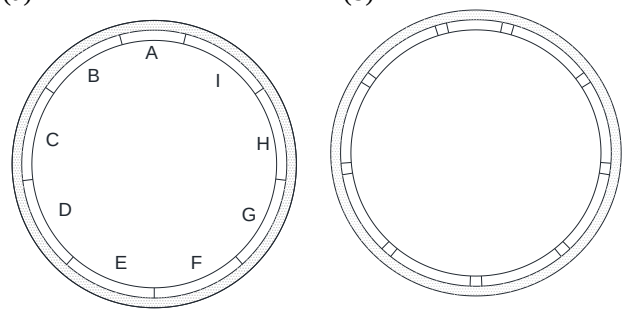

Fig. 3.(a) Segmental lining of Metro Line 6; (b) Numerical model in Plaxis 2D.

Figure 3(b) shows the numerical model adopted to simulate the semi-rigid behavior of longitudinal joint, capable to transmit axial force, shear force and bending moments. The joint is a deformable volume, with same thickness of the segment, whose stiffness is equivalent to that of a joint with a specific value of contact area, usually 2/3 to 3/4 of the segment thickness. The rotational stiffness is calculated at the 80% of maximum limit moment that can be transferred M_{pl}. The latter is calculated for an angle of rotation of 1%.

III. CASE OF STUDY OF NAPLES METRO LINE 6

Metro Line 6 has been excavated in a densely urbanized area of Naples with an earth pressure balance (EPB) machine, below the groundwater table.

The system support lining is the so called *universal ring*, 1.7m wide, assembled in nine precast concrete elements, eight segments with trapezoidal shape, corresponding to a central angle of 41.5 degrees, plus the keystone. The tunnel has an external excavation diameter of 8.135m, the lining has an intrados radius of 3.625m and extrados radius of 3.925m, for a total thickness of 0.3m, the annular void between the extrados and the external excavation diameter backfill with grout 0.1425m thick. The longitudinal connections are bi-block system, three for the main segment and one for the key.

The instrumented section is fully located in a sandy layer, 16.3m deep from the ground surface. Below the tunnel invert there is a layer of cineriti 8.4m thick overlying Neapolitan Yellow Tuff. The groundwater table is 6 m below ground level. Table 1 resumes the main soil parameters.

A. Instrumentations and monitoring data

Lining strains have been measured by means of vibrating wire gauges embedded in the concrete segments during their construction in the manufacturer's plant. Each segment of the ring has been instrumented with five pairs of extensometer bars, in transversal and longitudinal direction, arranged as in the Figure 4.

The measurements were recorded using a wireless data logger, which allowed an accurate follow up of the strain changes in the segments since the concreting stage, during installation and for a long time after the tunnel construction.

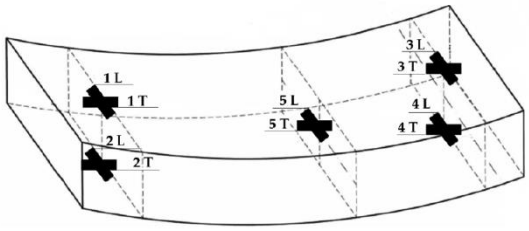

Fig. 4. Vibrating wire gauges layout.

The vibrating wire gauges measure indeed the variation of tensile stress Δσ of the wire as the variation of its natural frequency of vibration Δf due to the relative displacements at the ends of the strain gage. The deformations Δε are derived from Δσ as:

$$\Delta\epsilon = \frac{\Delta\sigma}{E} = \frac{1}{E}\frac{\rho}{4L^2}\Delta f^2 = k_e \Delta f^2 \qquad (1)$$

where E is the Young's modulus of the steel wire.

Since the steel wire and the concrete have different thermal expansion coefficients, due to an increase of temperature slacking of the wire may occur, hence the deformations calculated through Eq. (1) may need to be corrected [11].

Figure 5 shows, as an example, the time histories of

strain measured in the segment C (Figure 3a) of the instrumented ring, starting from its assembly inside the shield. It may be noticed that the measured strains increase significantly due to the jacking forces applied longitudinally to the lining ring, inducing strains of a few hundreds of $\mu\varepsilon$; the thrusted gauges are under compression while the lateral gauges dilate for Poisson effect.

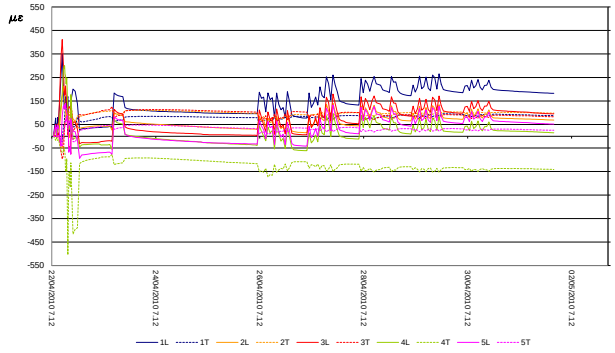

Fig. 5. Deformations of segment C [12].

B. Numerical simulations

A plane strain transversal section of the tunnel is shown in Figure 6; the layered soil has been modelled with Hardening Soil Small Strain constitutive model available in Plaxis 2D, using the parameters shown in Table 1 for sand and cineriti. The Neapolitan Yellow tuff has been modelled instead using the elastic-perfectly plastic Mohr Coulomb model, with parameters shown in Table 1.

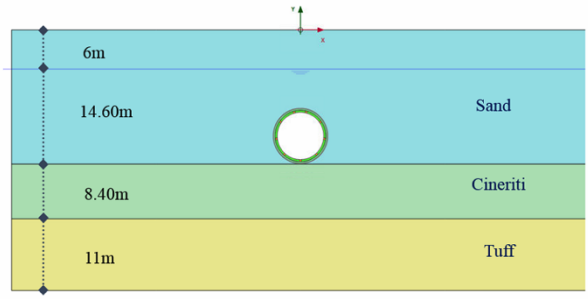

Fig. 6. Numerical 2D model.

The calibration of the segmental lining model has been carried out starting by the evaluation of the average value of axial forces N on the continuous lining, through the approach described before [13]. For a N_{av} equal to 750 kN/m, a joint contact area of 0.30m and a rotational stiffness k_θ = 48kNm/m has been calculated and an equivalent elastic Young modulus of the deformable volume of $6e^6$ kN/m^2. Table 2 resumes the lining parameters, considering an elastic behaviour of concrete segments, an elastic behaviour of longitudinal joints (under the hypothesis that under static loads they do not reach the plastic moment M_{pl}), elastic behaviour of the grout in the fresh state and in the hardened state.

Table 1. Ground properties and constitutive models calibration.

		Sand	*Cineriti*	*Tuff*
γ_{unsat}	kN/m^3	15	14	14
γ_{sat}	kN/m^3	18	16	16
v	-	0.3	0.3	0.3
φ	°	37	37	27
c'	kN/m^3	0	0	500
E	kN/m^2	$50e^3$	$40e^3$	$6.30e^6$
E^{50}_{ref}	kN/m^2	$40e^3$	$47e^3$	-
E^{oed}_{ref}	kN/m^2	$40e^3$	$47e^3$	-
E^{ur}_{ref}	kN/m^2	$85e^3$	$100e^3$	-
$\gamma_{0.7}$	-	$0.13e^{-3}$	$0.19e^{-3}$	-
G_0^{ref}	kN/m^2	$88e^3$	$182e^3$	-
p_{ref}	kN/m^2	115	170	-
m	-	0.5	0.5	-

Table 2. Lining Parameters.

	E kN/m^2	γ kN/m^3	v
Concrete	$38.25e^6$	25	0.2
Joint	$6e^6$	25	0.2
Fresh grout	$5e^3$	15	0.2
Hardened grout	$10e^6$	15	0.2

In order to reproduce the initial state of stress around the tunnel, taking into account the 3D arching effect that occurs within the soil and the deformations that occur around the unsupported cavity, the so-called Converge-Confinement Method has been adopted for which the initial stress acting on the cavity is equal to:

$$\sigma = (1-\lambda)\,\sigma_0 \qquad (2)$$

For the reference case a value of the stress relaxation coefficient $\lambda = 0.3$ has been used. This means that the real state of stress acting on the lining is 70% of the total load. This value [12] has been calibrated in such a way that the volume loss of numerical simulation was equal to that measured on site.

The de-confinement process modelling excavation has been then performed into four phases:

1. Generation of the initial stress field;
2. Plastic calculation to carry out an elastic-plastic deformation analyses in drained conditions with the application of CC-method;
3. Plastic calculation to carry out an elastic-plastic

deformation analyses in drained conditions of the lining installation and grouting;

4. Plastic calculation in drained condition to evaluate the deformations when the grout is hardened.

It is important to consider the two states of the grout when interpreting the deformation measures of monitoring data. In fact when the grout is in the fresh state, it is possible to imagine an interaction condition between grout and sandy soil very close to *full-slip* condition. Vice versa, when the grout is in the hardened state, the same condition is very close to that of a *no-slip* interface.

For these reasons in the face three of the excavation process, an interface surface has been applied between sand and fresh grout with $R_{interface}$= 0.3, to reproduce a slip condition, another interface between concrete lining and fresh grout simulates the relative movement ($R_{interface}$ = 0.3).

In the last calculation phase the grout-soil interface was set to $R_{interface}$=0.7, while the concrete-grout interface was set to $R_{interface}$ =0.9, to model an almost no-slip condition.

Figure 7(a) e (b) shows influence of joints on the structural behaviour of lining.

In terms of bending moments, the effect of joints implies a reduction of the absolute maximum and minimum value of about 30kN/m; in terms of normal forces there are oscillations of the average value in correspondence of joint locations in a range of ±100kN/m.

(a)

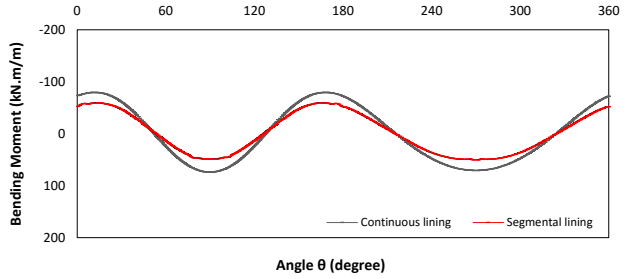

(b)

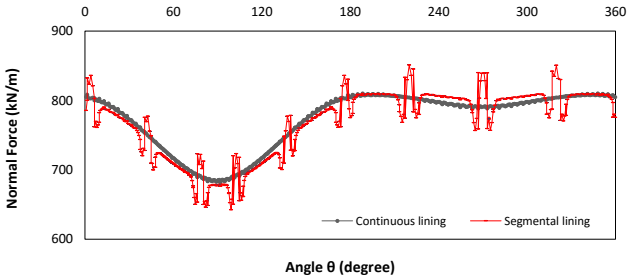

Fig. 7. (a) Comparison results of bending moments M in continuous lining and in segmental lining; (b) Comparison results of axial forces N in continuous lining and in segmental lining.

The difference in the maximum absolute bending moments between continuous and segmental lining increases when the joint number increases; this is due the fact that the span of each segment become shorter by increasing the segments number [13].

Of course, such considerations refer to a specific technology of joints, with a specific relative stiffness and a specific contact area.

In order to compare the results in terms of deformations, Tables 3 to 10 show the transversal component of numerical deformation of the nodes corresponding to the transversal vibrating wire gauges location (Figure 4) in the segments C to I (Figure 3(a)).

Table 3. Comparison of measured and calculated deformation of segment C.

ε (10^{-3})	*Measured*	*Calculated*
1 T	*0.180*	0.040
2 T	*0.80*	0.090
3 T	*0.80*	0.050
4 T	*-0.150*	0.102
5 T	*0.015*	0.050

Table 4. Comparison of measured and calculated deformation of segment B.

ε (10^{-3})	*Measured*	*Calculated*
1 T	*0.250*	0.072
2 T	*-0.050*	0.051
3 T	*0.180*	0.015
4 T	*0.02*	0.078
5 T	*-0.010*	0.051

Table 5. Comparison of measured and calculated deformation of segment D.

ε (10^{-3})	*Measured*	*Calculated*
1 T	*0.100*	0.07
2 T	*-0.010*	0.06
3 T	*0.070*	0.10
4 T	*-0.120*	0.035
5 T	*0.070*	0.067

Table 6. Comparison of measured and calculated deformation of segment E.

ε (10^{-3})	*Measured*	*Calculated*
1 T	*0.150*	0.031
2 T	*-0.010*	0.126
3 T	*-0.010*	0.056
4 T	*-0.070*	0.043
5 T	*-0.050*	0.086

Table 7. Comparison of measured and calculated deformation of segment F.

ε (10^{-3})	*Measured*	*Calculated*
1 T	*-0.050*	0.043
2 T	*-0.030*	0.086
3 T	*0.010*	0.007
4 T	*-0.100*	0.090
5 T	*0.100*	0.089

Table 8. Comparison of measured and calculated deformation of segment G.

ε (10^{-3})	*Measured*	*Calculated*
1 T	*0.100*	0.094
2 T	*0.050*	0.007
3 T	*0.130*	0.071
4 T	*0.350*	0.060
5 T	*0.050*	0.050

Table 9. Comparison of measured and calculated deformation of segment H.

ε (10^{-3})	*Measured*	*Calculated*
1 T	*-0.100*	0.106
2 T	*0.000*	0.018
3 T	*0.090*	0.139
4 T	*0.010*	0.007
5 T	*-0.270*	0.056

Table 10. Comparison of measured and calculated deformation of segment I.

ε (10^{-3})	*Measured*	*Calculated*
1 T	*-0.020*	0.012
2 T	*0.070*	0.064
3 T	*0.080*	0.063
4 T	*-0.430*	0.043
5 T	*-0.020*	0.056

Calculated deformations are in some cases one order of magnitude lower than the measured ones. This result should not be unexpected, since the plane strain numerical model indeed is not able to reproduce the 3D excavation process and in particular the jacking thrust effect in longitudinal directions, which tends to increase the deformations as the time history of deformations in Figure 5 shows.

Figure 8(a) e (b) shows the results obtained by Marino [12] in term of transversal bending moments and axial forces. The value have been back-analysed from the measured micro-strains in the hypothesis of lining section resistant to tensile stress up to admissible limiting strain of 50με. Also in terms of forces the results obtained by plane strain analyses are lower than measured.

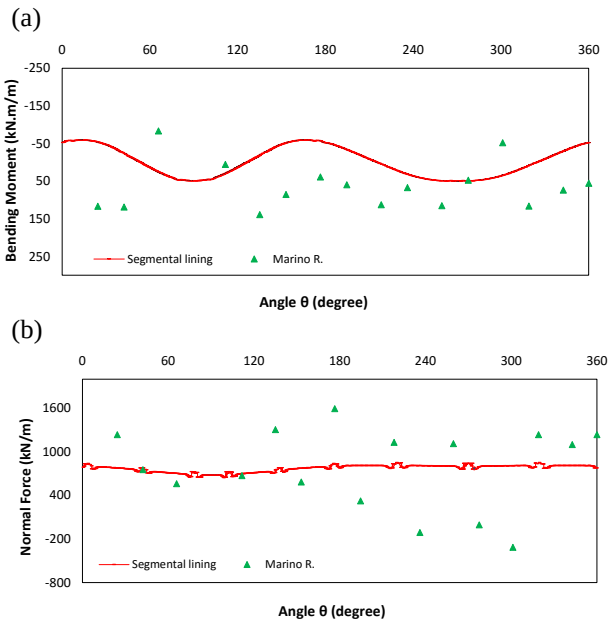

Fig. 8. (a) Back-analysed transversal bending moments M [12]; (b) Back-analysed axial forces N [12].

IV. CONCLUSIONS

A 2D numerical analyses has been performed to study the effect of the segmental nature of the lining and the interaction mechanism between concrete-grout-soil on the

behavior of a tunnel support system in order to interpret the monitoring data of an instrumented ring. The results show that the segmental lining model involves a not negligible variation in the structural forces, the necessity of consider the grout in the fresh state in order load realistically the lining ring, which otherwise would be underestimated. A plane strain model however is not able to investigate the impact of the entire excavation process, in particular the effect of jacking thrusts. The latter induce an increment of structural forces in the longitudinal direction neither it is able to model the circumferential joints, which imply a coupling effect between the segments in both directions thus providing a stiffer response of the lining. Three-dimensional numerical analyses are currently going on to simulate the real 3D structure of lining, the real excavation process, and to the interaction mechanism between concrete-fresh grout-soil.

ACKNOWLEDGEMENTS

The activity was carried out as part of WP 3 'Tunnels' of the sub-project on 'Earthquake Geotechnical Engineering', in the framework of the research programme funded by Italian Civil Protection through the ReLUIS Consortium.

REFERENCES

[1] Wood, A. M., *The circular tunnel in elastic ground.* Geotechnique, *25*(1), 115-127 (1975).

[2] N.A. Do, D. Dias, PP. Oreste, I.Djeran-Maigre, "*A new numerical approach to the hyperstatic reaction method for segmental tunnel linings*", Int. J. Numer. Anal. Meth. Geomech. (2014). 28(15) 1617–1632.

[3] CB. Bloom, "*Design philosophy of concrete linings for tunnel in soft soils*". Ph.D. dissertation, (2002), Delft University, Netherlands.

[4] Ding W.Q.,Yue Z.Q., Tham L.G., Zhu H.H., Lee C.F., hashimoto T., "*Analysis of shield tunnel. International*". (2004). Journal for Numerical and Analytical Methods in Geomechanics 28, 57-91.

[5] O. Arnau, C. Molins, "*Three dimensional structural response of segmental tunnel lining*", Eng. Struct. (2012) 44:210-221.

[6] N.A. Do, D. Dias, PP. Oreste, I.Djeran-Maigre,"*Three-dimensional numerical simulation for mechanized tunneling in soft ground: the influence of the joint pattern*". Acta Geotechnica (2013) DOI 10.1007/s11440-013-0279-7.

[7] Kartal M.E., Basaga H.B., Bayraktar A. Muvafik M., "*Effects of semi-rigid connection on structural responses".* Electronic journal of structural engineering. (2010) 10:22-35.

[8] Janssen, P., *"Tragverhalten von Tunnelausbauten mit Gelenktübbings".* (1983). Report No. 83-41 University of Braunschweig". Department of civil engineering, Institute for structural analysis.

[9] F. Leonhardt, H. Reimann. Betongelenke. Der Bauingenieur 41 (1966), No 2, pp. 49-56.

[10] Plaxis 2D Reference manual 2015.

[11] G. Pepe, "*Rivestimenti di gallerie in conci prefabbricati: sperimentazione e analisi".* Ph.D. dissertation, (2008), University of Naples, Federico II.

[12] R. Marino, "*Misure di deformazione nei rivestimenti di gallerie metropolitane".* Ph.D. dissertation, (2010), University of Naples, Federico II.

[13] C. Thienert, M. Pulsfort, "*Segments design under consideration of the material used to fill the annular gap*". Geomech Tunn (2011) 4:665-679 gap".

[14] N.A. Do, D. Dias, PP. Oreste, I.Djeran-Maigre, "*2D numerical investigation of segmental tunnel lining*". Tunnelling and Underground Space Tecnology 37 (2013) 115-127.